Multinuclear Magnetic Resonance and DFT Studies of the Poly(chlorotrifluoroethylene-alt-ethyl vinyl ether) Copolymers

ARTICLE *in* MACROMOLECULES · AUGUST 2009

Impact Factor: 5.8 · DOI: 10.1021/ma900789t · Source: OAI

4 AUTHORS, INCLUDING:

Diego Carnevale
Université de Neuchâtel
26 PUBLICATIONS **273** CITATIONS

5652 *Macromolecules* **2009**, *42*, 5652–5659
DOI: 10.1021/ma900789t

Macromolecules
ARTICLE

Multinuclear Magnetic Resonance and DFT Studies of the Poly(chlorotrifluoroethylene-*alt*-ethyl vinyl ether) Copolymers

Diego Carnevale,[†] Philip Wormald,*[,†] Bruno Ameduri,[‡] Russell Tayouo,[‡] and Sharon E. Ashbrook[†]

[†]*School of Chemistry, University of St. Andrews, Purdie Building, St. Andrews KY16 9ST, Scotland, and* [‡]*Ingénierie et Architectures Macromoléculaires, Institut Charles Gerhardt - UMR(CNRS) 5253 Ecole Nat Sup de Chimie de Montpellier 8, Rue de l'Ecole Normale, 34296 Montpellier, France*

Received April 10, 2009; Revised Manuscript Received June 19, 2009

ABSTRACT: Chlorotrifluoroethylene (CTFE) and ethyl vinyl ether (EVE) were reacted under radical conditions to produce the poly(CTFE-*co*-EVE) alternating copolymer, and a full ^{13}C, ^{1}H, and ^{19}F NMR structural interpretation is offered. All spectra were characterized by broad signals resulting from the overlapping of different chemical shifts. This observation was rationalized by considering a complex mixture of diastereomerically related compounds, hence allowing an average assignment to be determined. A density functional theory (DFT) computational study of the isotropic magnetic shieldings with the GIAO and CSGT methods was performed to explore the diasteriomeric relationships between the single building blocks and their mutual influences along the polymer chain. The calculated results totally support the assignment of the experimental chemical shifts of two diasteriomeric sets of resonances indicating chiral center inversion, and not spin−spin *J* coupling interactions, as the main cause of spectral complexity.

Introduction

Fluoropolymers are well-known for their high-performance features, i.e., heat and chemical resistance, low refractive index, low surface energy, and durability,[1] and therefore have a wide area of applications, e.g., paints, actuators, transducers fuel cell membranes, optical fibers, thermal and surface active coatings, gaskets, O-ring, insulating wires, and textiles finishings They have been usually obtained by radical copolymerization of fluoromonomers. Among them, poly(chlorotrifluoroethylene), PCTFE, was the first fluoropolymer, discovered in 1934, and has valuable properties, with exceptional gas and moisture barrier properties. However, because of its high crystallinity rate, PCTFE is hardly soluble is common organic solvents and only in dichloropolyfluorobenzene, which is why the copolymerization of two or three comonomers is of specific interest, offering the possibility of enhancing polymer properties and tailored design for specific applications. The radical copolymerization of CTFE with vinyl acetate, styrene, and methyl methacrylate was first reported by Thomas and O'Shaughnessy,[2] leading to statistical copolymers with a lower reactivity of CTFE than those of the comonomers. Later on, the copolymerization of CTFE with ethylene and propylene has also been reported and was interestingly shown to proceed in an alternating manner by Garbuglio et al.[3] Alternating copolymerization of fluoro-olefins and vinyl ethers was first carried out by Tabata in 1971.[4] From these early experiments a new range of soluble, room temperature curing, amorphous copolymers were developed, leading to a new type of paint resin commercialized under the Lumiflon[5−7] trade name, as reviewed by Takakura.[8] However, NMR studies of these important CTFE-containing fluoropolymers have proven difficult to decipher due to the broad unresolved lines observed in the ^{1}H, ^{13}C, and ^{19}F NMR spectra, obstructing the determination of $^{1}H-^{19}F$ coupling constants and detailed structure of the copolymer. Furthermore, few detailed analyses using multinuclear ^{19}F, ^{13}C, and ^{1}H NMR spectroscopy for the copolymerization products of CTFE and ethyl vinyl ether (EVE), which may aid structural determination, have been found in the literature.[9]

In comparison, homopolymers such as PVDF have been extensively studied by NMR, and both homo- and heteronuclear $J_{F,F}$, $J_{H,H}$, and $J_{F,H}$ coupling constants have been reported. The problem of resolution and subsequent signal assignment for fluoropolymers polymers is often complicated because analyses are often carried out on samples of raw synthetic samples, which contain a mixture of reaction products, i.e., with varying chain lengths, and many possible functional end chain groups.[10−12] Multinuclear NMR correlation experiments on samples related to fluoropolymers to gain resolution for a specific group of signals in the polymer have been published,[13−15] but their assignments are often deduced from spectra of model compounds or samples obtained from a variety of synthetic pathways.[10,11,16−18] We have recently demonstrated that this can be achieved using multinuclear NMR and the main chain structure, end groups, and byproducts can be sufficiently analyzed and reported new $^{1}H-^{19}F$, $^{1}H-^{1}H$, and $^{19}F-^{19}F$ coupling constants for a VDF telomer.[19] For the observation of small coupling constants, resolution is obviously of great importance, which is the main reason why $^{3}J_{F,F}$ and $^{4}J_{H,H}$ couplings are seldom seen in spectra of high molecular weight polymers in general, often having line widths greater than 10 Hz. It should also be noted that the $^{n}J_{F,F}$ couplings do not follow the same general behavior as $^{n}J_{H,H}$ couplings.[20] It is possible for groups in straight-chain fluorinated compounds to have vicinal $^{3}J_{F,F}$ couplings near to zero, whereas $^{4}J_{F,F}$ coupling constants can be quite large, ∼10 Hz.[21] Hence, care must be taken when assigning coupling constants and thereby determining the structure of fluorinated compounds. Furthermore, ^{19}F COSY spectra can often give more correlations than are typically found in a ^{1}H COSY spectrum due to overlapping electron distribution of two fluorines in close proximity,

*Corresponding author: Tel +44-(0)1334-453382; Fax +44-(0)1334-453808; e-mail pw22@st-andrews.ac.uk.

 Published on Web 07/09/2009

thereby allowing correlation of electron and nuclear spins in addition to electron pair bond to electron pair bond via the molecular framework.[20,22] While many examples of $^{1}H-^{19}F$ heteronuclear correlation experiments have been published,[23,24] relatively few have been applied to hydrogen-containing polymeric fluorine systems. With respect to the copolymerization of CTFE with VDF, NMR has shown that the CTFE is exclusively attacked by the CF_2 group giving tail-to-tail placements. ^{19}F NMR showed that the microstructure of the poly(VDF-*co*-CTFE) copolymer was dominated by VDF−VDF (head to tail) and VDF−CTFE (tail to tail) structures.[25] Using this knowledge, we now turn our attention to the structure of the poly(CTFE-*co*-EVE) copolymer, where previous NMR work on this polymer[9] concluded that a full structural analysis was not possible, and only the assignments of the proton signals of the ethyl ether side chain were established. Furthermore, ^{19}F spectroscopy resulted in a very complex spectrum, which could not be not substantially analyzed either. No extensive investigation using one- and two-dimensional solution-state NMR experiments on chlorotrifluoroethylene (CTFE) and ethyl vinyl ether (EVE) copolymers appears to have been carried out hitherto. Therefore, this paper reports the characterization of products arising from the radical copolymerization of CTFE with EVE in ethyl acetate by ^{19}F, ^{13}C, and ^{1}H solution-state NMR spectroscopy to evaluate structure and report coupling constants where possible, verify our findings using density functional theory, and debate these results in terms of stereochemistry.

Experimental Details

Chlorotrifluoroethylene (CTFE) was kindly supplied by Honeywell, Morristown, NJ, and Buffalo, NY, *tert*-butyl peroxypivalate by Akzo Nobel, and acetonitrile by SDS and were used as received. The structures of the copolymers were determined by NMR spectroscopy at room temperature. All NMR data acquisition was performed using the standard Bruker software (Topspin 2.0). All NMR spectra were obtained using a Bruker Avance II 400 (9.4 T) equipped with a triple-resonance indirect detection probe. The solvent was chosen to be $CDCl_3$, and the solutions were prepared directly into 5 mm NMR tubes; all spectra were acquired at 25 °C. ^{1}H NMR 400.1 MHz, $CHCl_3$ at 7.29 ppm as internal standard, 30° flip angle (4.16 μs), 1.0 s relaxation delay, 0.3 Hz line broadening, and 65K data points acquired. ^{13}C NMR 100.5 MHz, $CDCl_3$ at 77.0 ppm as internal standard, 30° flip angle (4.23 μs), 2.0 s relaxation delay, 2.0 Hz line broadening, and 65K data points were acquired. ^{19}F NMR 375.5 MHz, $CFCl_3$ at 0.0 ppm as internal standard, 30° flip angle (2.83 μs), 1 s relaxation delay, 0.3 Hz line broadening, and 131K data points were acquired. For the ^{1}H COSY and ^{19}F COSY, 2048 data points and 256 increments (direct and indirect dimensions, respectively) were acquired; a sine-bell window function was applied to both dimensions. For the $^{1}H-^{13}C$ HSQC, 1024 data points and 256 increments were acquired, a 90° shifted squared sine-bell window function was applied to both dimensions, and a 3.45 ms coherence-transfer delay was used. For the $^{1}H-^{13}C$ HMBC, 2048 data points and 256 increments were acquired, a sine-bell window function was applied to both dimensions,and a 62.5 ms coherence-transfer delay was used. For the $^{1}H-^{19}F$ HMQC, 1024 data points and 128 increments were acquired, a 45° shifted squared sine-bell window function was applied to both dimensions, and a 55.6 ms coherence-transfer delay was used. For the ^{19}F J-res, 4096 data points and 128 increments were acquired, and a sine-bell window function was applied to both dimensions. For the $^{1}H-^{13}C$ HSQC, 1024 data points and 256 increments were acquired, a 90° shifted squared sine-bell window function was applied to both dimensions, a 3.45 ms coherence-transfer delay was used, and phase sensitivity was achieved using echo/antiecho gradient selection. Size exclusion chromatography (SEC) analyses were performed with a Spectra-Physics apparatus equipped with two PLgel 5 μm Mixed-C columns from Polymer Laboratories and a Spectra-Physics SP8430 refractive index (RI) detector. Tetrahydrofuran (THF) was chosen as the eluent at $T = 25$ °C, with a flow rate of 0.8 mL min^{-1}. Monodisperse standards were poly(styrene), purchased from Polymer Laboratories. Differential scanning calorimetry (DSC) measurements were conduced using a TA 2920 analyzer from TA Instruments DA 73085, a RCS DA cooler, and Sartorius MC5 weighing machine. Scans were recorded at a heating rate of 10 °C min^{-1} from −50 to 180 °C. The T_g value was taken in the second scan as the inflection point in the heat capacity jump.

Scheme 1. Structure of Chlorotrifluoroethylene (CTFE) Showing Three Nonequivalent Fluorine Atoms

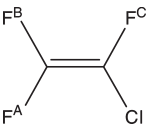

Radical Copolymerization of CTFE with Ethyl Vinyl Ether. In a 300 cm^3 Hastelloy autoclave equipped with a manometer, a magnetic stirrer, and safety inlet and outlet valves, 1.194 g (6.86 mmol) of *tert*-butyl peroxypivalate as the initiator, 18.57 g (0.257 mol) of ethyl vinyl ether, and 150 mL of dry acetonitrile were introduced and purged with argon for 15 min. The vessel was closed and checked for the leak at 30 bar of nitrogen. The reactor was placed in acetone/liquid nitrogen to cool the contents. Subsequently, 5−7 vacuum−argon cycles were applied to remove oxygen from the liquid. The required amount of CTFE (30 g, 0.257 mol) was condensed in the autoclave and assessed by double weighing. Then, the autoclave was heated up to 74 °C. The pressure reached a maximum of 6 bar, and then a sharp decrease to 1 bar in the pressure at almost constant temperature (74 °C) for the first hour was observed. The radical copolymerization was still carried out at that temperature for an additional 4 h, and no decrease of pressure was noted. After the reaction stopped, the autoclave was cooled and then placed in an ice bath. The unreacted monomer was expelled by purging, and the conversion of copolymerization was determined by double weighing (∼75%). After opening the autoclave, acetonitrile was evaporated, and the total product was precipitated from a large excess of methanol. This procedure was carried out twice. After filtration and drying at 50 °C under 1 mbar, a brown solid was obtained with a molecular weight of ca. 23 000 g mol^{-1} (PS standards) and polydispersity index of 2.5. The glass transition temperature (T_g) was 19 °C.

Computational Methods. Calculations were carried out using the Gaussian03 package[26] on the EaStCHEM research computing facility on a four-processor single node. Structures were optimized with the DFT B3LYP hybrid functional and the 6-31G+(d) basis set. Both the GIAO and CSGT methods were then used for the calculations of the isotropic magnetic shieldings on these structures using the same level of theory. The calculated shielding references were chosen to be $CFCl_3$ for fluorine and $CHCl_3$ for both proton and carbon.

Results and Discussion

Spectroscopy of Main-Chain Units. The ^{19}F chemical shifts of the free CTFE (Scheme 1) have been reported previously[27,28] with F^A, F^B, and F^C at −118.9, −101.4, and −143.5 ppm, respectively. Furthermore, the mechanism of the acceptor−donor alternating copolymerization of CTFE with vinyl ethers (Scheme 2) has also been investigated.[1−4,8,9,28]

The reaction of EVE with CTFE is shown in Scheme 2; the copolymer is formed from the free monomers on the evaluation of ^{1}H and ^{13}C NMR spectra and elemental analysis[9,27,28]

Scheme 2. Simplified Mechanism of the Synthesis of Poly(CTFE-*alt*-VE) Copolymer

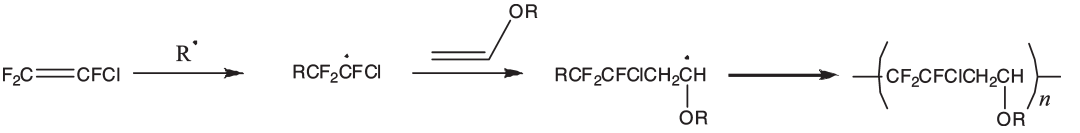

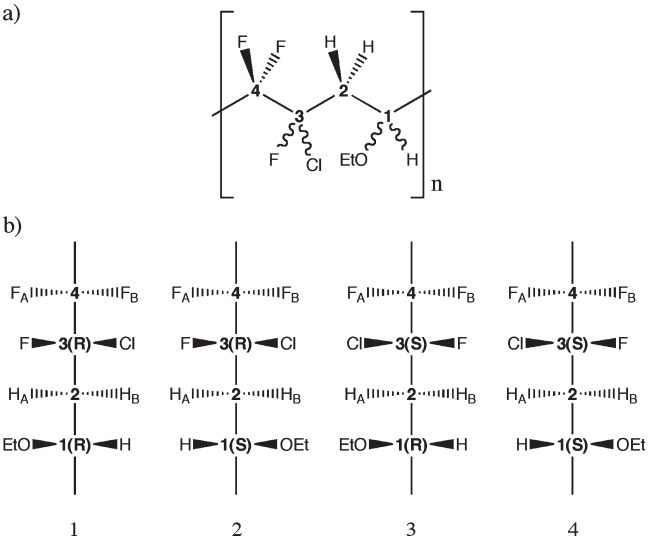

Figure 1. Chiral repeating unit of the CTFE/EVE polymer showing carbons 1, 2, 3, and 4 of the backbone (a) and the Fischer projections of four possible diastereoisomers (1, 2, 3, and 4) of the monomer (b).

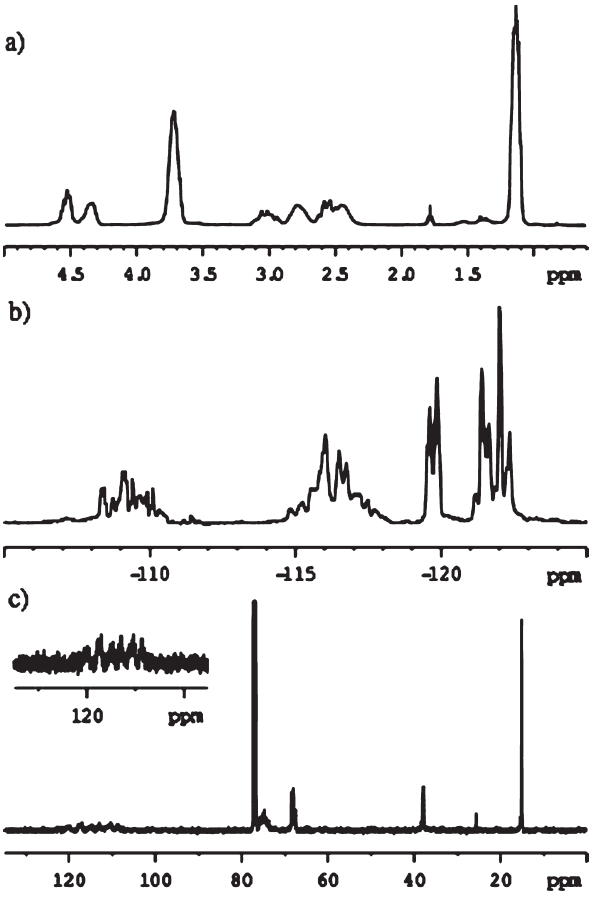

Figure 2. 400 MHz (a) ^{1}H (^{19}F decoupled), (b) ^{19}F (^{1}H decoupled), and (c) the ^{13}C (^{1}H decoupled) NMR spectra of CTFE/EVE polymer in $CDCl_3$.

which confirmed the alternated structure of the resulting poly(CTFE-*co*-EVE) copolymer.

Considering the structures in Figure 1a, it should be noted that carbons 1 and 3 are chiral. This results in four possible diastereoisomers for a single repeating unit. Analyzing the Fischer projections of these in Figure 1b, it appears clear that the diastereoisomer pairs (1, 4) and (2, 3) are enantiomers and that in a nonasymmetric environment such as $CDCl_3$ solution they will give rise to the same NMR spectra; i.e., 1 will be indistinguishable from 4 and 2 will be indistinguishable from 3. The diastereomeric relationships between the four chiral units are as follows: (1, 2), (1, 3), (2, 4), (3, 4). These four couples simply indicate the stereochemical relationships (see Figure 1b) between the four units and are not related to the physical sample, which is assumed to be made up of all 1, 2, 3, and 4 in a random manner. Therefore, in this case, the solution-phase NMR technique can only identify the system as made up of two molecules, which must be in diastereomeric relationship. For the purpose of assignment, one can postulate that the spectra are made up of only one of the four diastereomeric couples which we refer to as (A, B). As an alternative explanation, if we could record a spectrum S^i of each pure *i*th monomer, we would have S^1, S^2, S^3, and S^4. By virtue of the stereochemical relationships which occur between these monomers, we would find that $S^1 = S^4 = S^A$ and $S^2 = S^3 = S^B$. This again shows that, as it is experimentally observed, only two monomers can be distinguished by NMR.

The system is complicated further by the fact that, in a polymer, different combinations of these diasteriomeric building blocks are possible, with the number of combinations depending on the length of the polymer. All these factors will contribute to NMR spectra, which will be characterized by broad signals centered on an averaged shielding. Figure 2a represents the ^{1}H NMR spectrum in $CDCl_3$ of poly(CTFE-*co*-EVE) copolymer. Considering the integral values, the resonances at 4.63 and 4.45 ppm ($\Delta\nu_{1/2}$ = 30.5 and 39.7 Hz, respectively) can be attributed to the same proton in the two different A and B diastereoisomers. Their chemical shifts are consistent with the C(1)*H*, and the most shielded (4.45 ppm) is arbitrarily defined as being part of the A set of resonances. An analogous differentiation is experienced by the resonances between 2.4 and 3.3 ppm, consistent with the diastereotopic C(2)H_2. Both the methyl and the CH_2 group of the ethoxy group appear as broad signals resulting from overlap of resonances with slightly different chemical shifts. Proton acquisition with ^{19}F decoupling does not yield either considerable resolution enhancement or further information on proton homonuclear multiplicities. Figure 2b shows the ^{19}F (^{1}H decoupled) NMR spectrum. The acquisition of a proton-coupled ^{19}F spectrum did not reveal any significant change in the pattern of signals, therefore indicating the presence of different chemical shifts rather than multiplicity due to $^{n}J(^{1}H-^{19}F)$ coupling, to be the cause of the large line widths. This results in each of the three different ^{19}F nuclei being represented by a group of signals rather than well-resolved single peaks. The lack of a systematic overlap of resonances (in contrast with the ^{1}H case) reveals the ^{19}F shieldings to be much more sensitive to the random changes

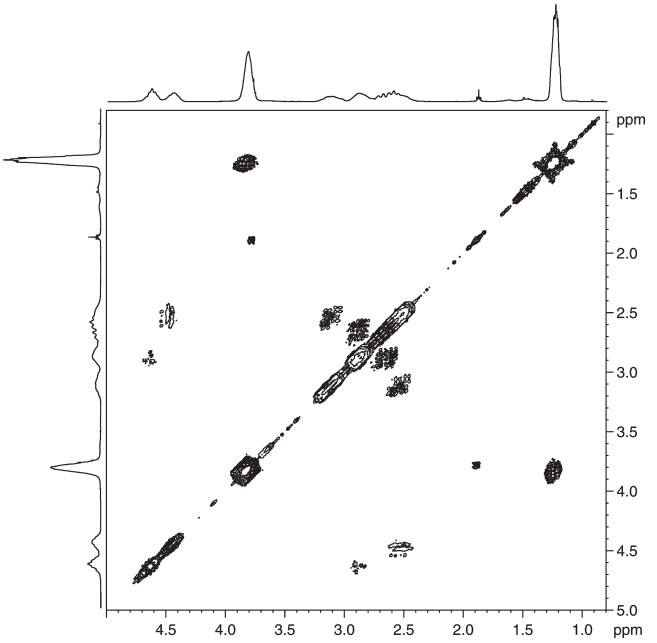

Figure 3. 400 MHz ^{1}H (^{19}F decoupled) COSY NMR spectrum of CTFE/EVE polymer in $CDCl_3$.

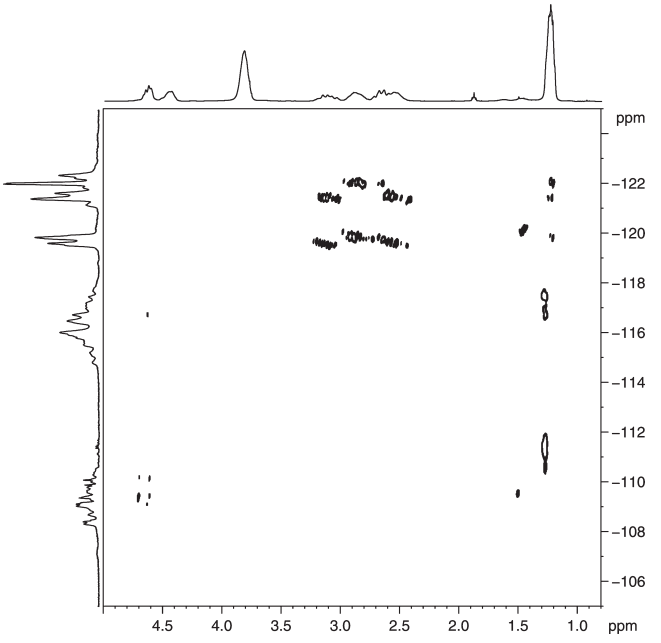

Figure 4. 400 MHz ^{1}H−^{19}F HMQC spectrum of CTFE/EVE polymer in $CDCl_3$.

in the sequence of units along the polymeric chain and, most importantly, prevents the identification of two clear A/B ^{19}F sets of resonances in the spectrum. It is also worth noting that no signal is seen for the CTFE−CTFE diad at −100 ppm[25] or −127 ppm.[27] The ^{13}C NMR spectrum of poly(CTFE-*co*-EVE) copolymer is shown in Figure 2c. The presence of $^{1}J(^{13}C-^{19}F)$ and $^{2}J(^{13}C-^{19}F)$ scalar couplings of ∼251 and ∼32 Hz, respectively, explains the multiplicity exhibited by the resonances at 117.5 and 110.1 ppm, which can be therefore assigned to C(4) and C(3). The chemical shift values for all nuclei are presented in Table 1 (Supporting Information). As expected, resonances appear to result from considerable overlap of several chemical shifts; therefore, it is not possible to distinguish between the two main sets of signals from these experiments. This problem is addressed later by applying a multiplicity edited ^{1}H−^{13}C HSQC (heteronuclear single quantum correlation) experiment.

The ^{1}H COSY (correlation spectroscopy) spectrum shown in Figure 3 provides discrimination of the two separate sets of resonances. The signals at 4.45, 3.12, and 2.52 ppm all correlate and are assigned to diastereoisomer A whereas the signals at 4.63, 2.89, and 2.63 ppm are assigned to diastereoisomer B. To distinguish between the several ^{19}F chemical shifts seen in Figure 2b and obtain the corresponding discrimination in the fluorine system as seen in the ^{1}H COSY spectrum (i.e., six resonances to assign, three for the A and three for the B diastereoisomers), a ^{1}H−^{19}F HMQC (heteronuclear multiple quantum correlation) spectrum (Figure 4) was acquired. The four A/B C(2)H_2 resonances between 2.4 and 3.3 ppm, correlate with four ^{19}F resonances between −119 and −123 ppm coherently with the two ^{1}H spin systems (none of these ^{19}F resonances correlate with both the A/B set of proton resonances). The fluorine resonance at −109.4 ppm correlates with the C(1)*H* at 4.63 ppm (B set). The ^{19}F resonance at −115.8 ppm does not show such a clear correlation in the spectrum, but by virtue of the restriction of the ^{1}H spin system, it must be included in the A diastereoisomer set of resonances, despite the lack of correlation with the C(1)H at 4.45 ppm. The correlations seen for ^{19}F groups of resonances with the CH_3 of the ethoxyl substituent (and yet

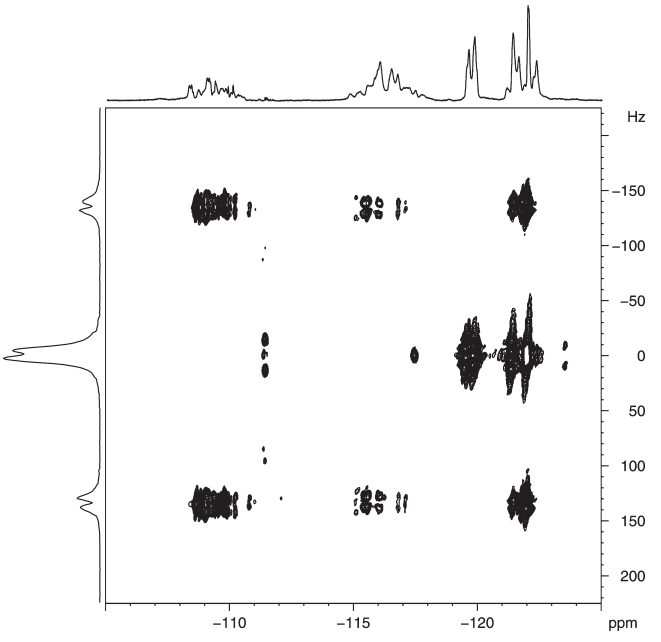

Figure 5. 400 MHz *J*-resolved ^{19}F NMR spectrum of CTFE/EVE polymer in $CDCl_3$.

none with the CH_2 of the ethoxyl) are not properly understood but could be the result of pseudo-coupling caused by electron sharing of the larger fluorine atom. As shown in Figure 4, and based on the assigned ^{1}H resonances, six ^{19}F resonances can be identified, i.e., three for the A and three for the B diastereoisomers, as expected.

As the two sets of proton signals from A and B have been distinguished via the ^{1}H COSY spectrum, the ^{1}H−^{19}F HMQC spectrum can therefore discriminate the two sets of three ^{19}F resonances. The possible presence of multiple-bond correlations such as those experienced by the CH_3, however, does not allow an unambiguous assignment of the fluorine resonances through the HMQC experiment, so a ^{19}F homonuclear *J*-resolved 2D experiment (Figure 5) was performed.

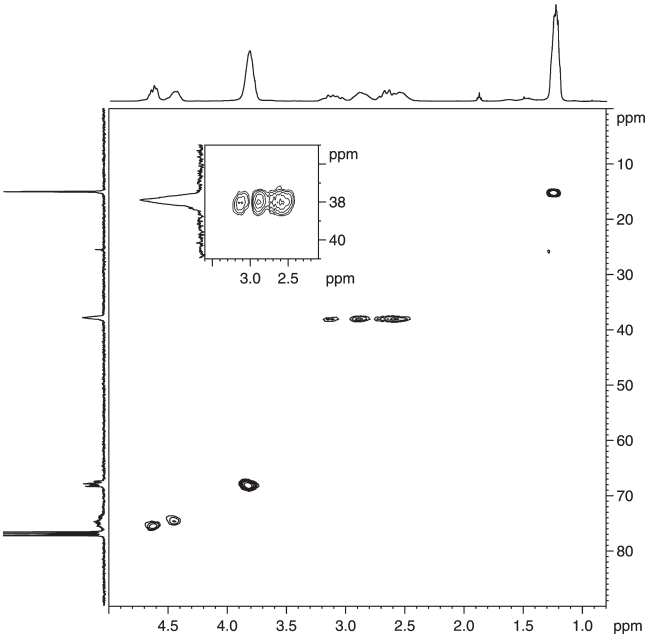

Figure 6. 400 MHz $^{1}H-^{13}C$ HSQC NMR spectrum of CTFE/EVE polymer in $CDCl_3$.

The four ^{19}F resonances centered at −109.4, −116.8, −121.4, and −122.0 ppm have a geminal coupling constant ^{2}J of ∼260−280 Hz. These must be therefore assigned to C(4)F_2 for A and B. The resonances at −119.6 and −119.9 ppm are characterized by a ^{3}J homonuclear coupling constant of ∼4−26 Hz and are therefore assigned to C(3)*F*. It should be noted that resonances at −121.4 and −122.0 ppm also retain the ^{3}J splitting, indicating that this fluorine in both A and B diastereoisomers has an associated dihedral angle with C(3)*F* that does not remove the coupling mechanism, as for ^{19}F at −109.4 and −116.8 ppm. Both ^{19}F chemical shifts and coupling constant values are in good agreement with the literature.[9,29−32] The spread of chemical shifts for each fluorine species, together with random overlap of resonances, does not allow multiplicities to be resolved even in the indirect dimension. A multiplicity edited $^{1}H-^{13}C$ HSQC (heteronuclear single quantum correlation) spectrum of the polymer is shown in Figure 6. From this $^{1}H-^{13}C$ single-bond correlation, it is possible to distinguish two different carbon resonances at 74.5 and 75.4 ppm to be assigned to C(1) in A and B and so confirming that ^{1}H resonances at 4.63 and 4.45 ppm do not result from a single chemical shift. On the contrary, the spread in the proton dimension reveals C(2) at 38.0 ppm to be overlapped for the two diastereoisomers, indicating the electronic environment of this carbon is not affected by the configurational change of the C(1) and C(3) chiral centers. The total assignments of ^{1}H, ^{13}C, and ^{19}F for both A and B diastereoisomers of the poly(CTFE-*co*-EVE) copolymer are reported in Table 1 (see Supporting Information for all tables).

From the analysis of the ^{19}F (^{1}H decoupled) NMR spectrum in Figure 2b and considering the assignment given in Table 1 (Supporting Information), it is interesting to notice that one of the two C(4)F_2 nuclei for both A and B diastereoisomers (−109.4 and −115.8 ppm, respectively) experiences a spread of chemical shift of ∼1250 Hz, whereas for all the other fluorine resonances a smaller spread of ∼90 Hz is observed. Therefore, one of the two C(4)F_2 nuclei seems to be particularly sensitive to the changes of electronic environment due to the different combinations of diasteriomeric building blocks preceding and following it in the polymeric chain. In addition, the chemical shifts difference of about 7 ppm found between these two resonances across the A/B couple is much larger than the ∼1 ppm difference found for all the others. These observations can be rationalized by considering that the configurational inversion in the C(1) (exchange of the position between the ethoxyl and the proton) of the following unit will produce a much larger change in the deshielding of the C(4)F_2 than that experienced by the C(3)*F* due to the configurational inversion of the C(3) (fluorine exchanged with a chlorine) for both electronic and steric considerations.

Computational Study. To reinforce the above assignment, a computational study was performed on a simplified system calculating the isotropic magnetic shieldings of ^{1}H, ^{13}C, and ^{19}F nuclei. Just like NMR in a nonasymmetric environment, also calculations in the vacuum cannot distinguish between enantiomers. This means that the couples (1, 4) and (2, 3) will give rise to the same structures and shieldings; i.e., if we calculate 1, then we do not need to calculate 4 (and vice versa), and if we calculate 2, then we do not need to calculate 3 (and vice versa). This means that only two structures (as long as they are one of the diastereomeric couples) need to be calculated to fully cover the whole stereochemical variety of the system. So, if for instance we chose 1, then we would need to calculate either 2 or 3. If we chose 2, then we would need to calculate either 1 or 4 and so on.

The less computationally demanding termination of the chosen single units with a group such as methyl has been considered too drastic a solution for the reliability of the shielding values of C(1) and C(4) in particular. Therefore, other units have been appended to both ends of the investigated central ones. These lateral units have been then terminated with methyls. Only the shieldings of the central units have been considered for the correlations with the experimental values assuming so that the methyl-termination approximation is in space and in number of bonds too far away for a non-negligible perturbation of the electronic density of the central units to take place. Structure 4 was chosen as the template central unit.

To explore the influences of the stereochemistry of the lateral units on the shieldings of the central one (4), two different lateral environments have been generated, (4−4−1) and (2−4−3). Once three-unit systems have been generated, the stereochemical relationships so far depicted and used as guidelines for a systematic and nonredundant study do not strictly stand anymore since they apply only to single units. This means that now we can investigate independently the effect of the inversion of configuration of the two chiral centers C(1) and C(3). The algorithm used to generate the structures is schematically represented in Figure 7 where the four systems are referred to as *a*, *b*, *c*, and *d*. The three-unit systems thus obtained allowed us to investigate the influence of different environments on a single unit (4 in *a* and *d*) and also the result of inversion of configuration of the two chiral centers C(1) and C(3) (*b* generated from *a* by inversion of C(3): (4→2) and *c* generated from *d* by inversion of C(1): (4→3)). Furthermore, the comparison between structures b and c (central units 2 and 3) yields information on how different lateral environments discriminate two units in an enantiomeric relationship which, in a single unit system, would have produced redundant data.

The four three-unit systems *a*, *b*, *c*, and *d*, were geometry optimized using the DFT B3LYP hybrid functional. The NMR shieldings were then calculated for the structures obtained with both the gauge-including atomic orbital (GIAO) and continuous set of gauge transformations

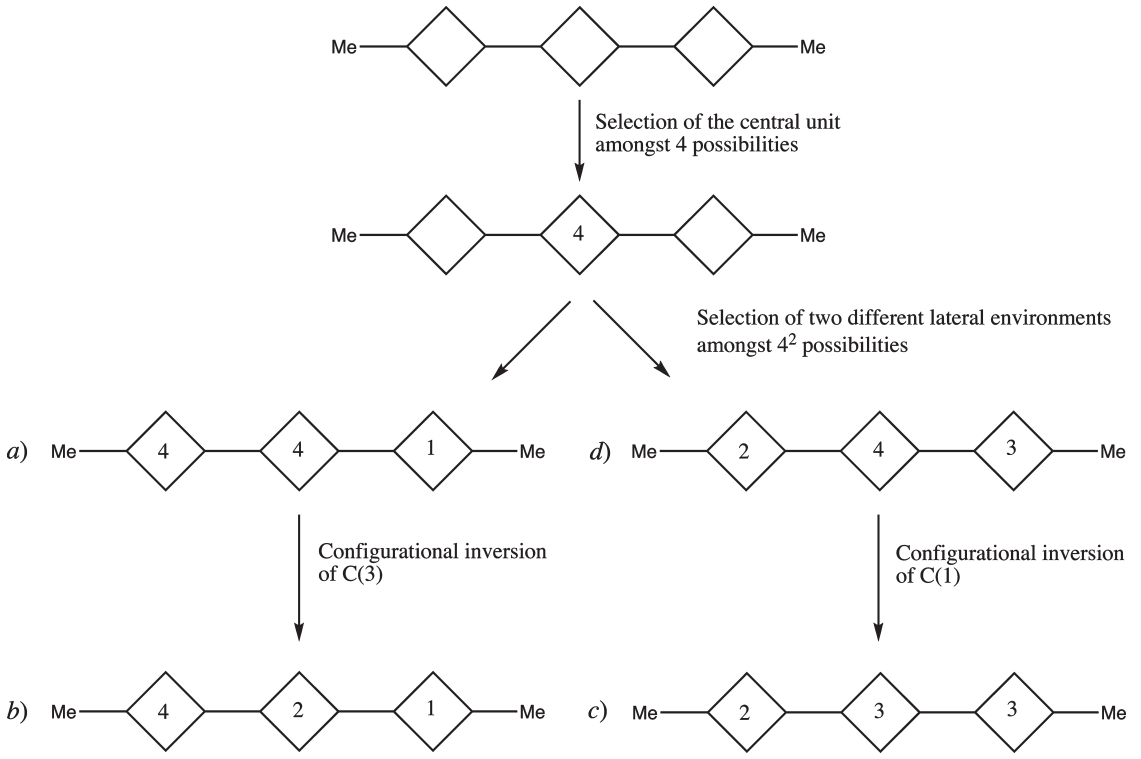

Figure 7. The four three-unit systems chosen to approximate the Gaussian calculations of the polymer along with the algorithm followed to generate them. The central units surrounded by the dashed box are in diastereomeric relationship.

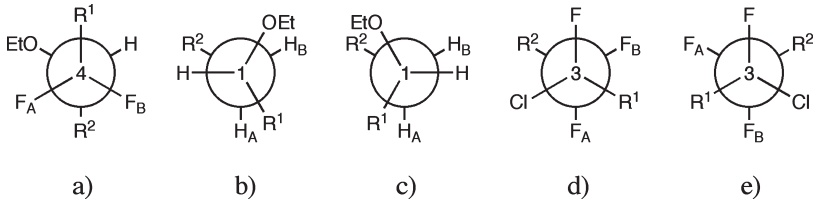

Figure 8. Newmann projections along the (a) C(4)−C(1) bond for *a*, *b*, *c*, and *d* as defined in Figure 7; (b) C(1)−C(2) bond for *a*, *b*, and *d*; (c) C(1)−C(2) bond for *c*; (d) C(3)−C(4) for *a*, *c*, and *d*; (e) C(3)−C(4) for *b*.

(CSGT) methods[33] at the same level of theory as the geometry optimization. The two methods are then compared in terms of average correlation coefficient $\overline{R^2}$ over the four calculated structures and an average computational error $\overline{\Delta\delta}$ defined as

$$\overline{\Delta\delta} = \frac{\sum_{i=1}^{n} \delta_i^{\mathrm{exp}}}{2} - \frac{\sum_{i=1}^{m} \delta_i^{\mathrm{calc}}}{4}$$

where n is the number of all the experimental resonances of the two diastereoisomers A and B (6 for ^{1}H and ^{19}F, 8 for ^{13}C) and m is the number of all the calculated shieldings of the four structures *a*, *b*, *c*, and *d* (12 for ^{1}H and ^{19}F, 16 for ^{13}C).

Analysis of ^{19}F NMR Computational Results. In agreement with the experimental assignment, both methods predict the C(3)*F* resonances to lie between the two C(4)F_2 resonances. In all of the three-unit systems considered, the ethoxyl group of the final unit is found in the Fisher projection (Figure 8) to be on the same side of the C(4)F_A. This fluorine is in fact predicted to be the most deshielded in all the four systems, thus proving the through-space deshielding effect of the oxygen nuclei[34] to be a determining factor in the ^{19}F shieldings. This is verified by considering the C(4)F_2 of the first unit of structure c, where the ethoxyl is on the same side of the C(4)F_B. This is the only unit where the order of shieldings of the two diastereotopic fluorines is inverted (i.e., F_B more deshielded than F_A). This coherent trend in the shieldings seems to be supported by the optimized geometries revealing how, along the C(4)−C(1) bond, the substituents adopt an almost ideal (average dihedral angle of 55.88°) staggered conformation in all of the structures considered (Figure 8). Furthermore, the most sterically hindering aliphatic substituents (R^1 and R^2) are always found in the expected *anti* positions, on an average dihedral angle of 178.82°. The experimental observation that only the less deshielded of the C(4)F_2 retain (in both A and B diastereoisomers) a homonuclear ^3J coupling with the vicinal C(3)*F* can be again rationalized considering the optimized geometries. In fact, whether it is F_A (in *a*, *c*, and *d*) or F_B (in *b*), all the structures are found in a staggered conformation across the C(3)−C(4) bond which determines the two dihedral angles (F_A−C(4)−C(3)−F and F_B−C(4)−C(3)−F) to be in all the cases very different, with average values of 72.30° and 173.30° (Figure 8d,e). The lack of a clear Karplus-type angular dependence of the $^3J_{FF}$ values upon the F−C−C−F dihedral angle[35] prevents a straightforward assignment of the diastereotopic C(4)F_2 on the basis of these computational results. All of the calculated structures seem to correlate better with

the experimental set of resonances for the B diastereoisomers ($R^2 = 0.999$ vs 0.942 for the GIAO/*a*, see Supporting Information). Nevertheless, the A pattern yields a slope of the correlation which approaches the unity (0.919 vs 0.389 for the GIAO/*a* case). The *a* structure (diastereoisomers 4 as central unit) displays the best correlation with both the experimental A and B sets of resonances, for both methods. Overall, although with a larger systematic error ($\overline{\Delta\delta}_{GIAO}$ = 28.6 ppm, $\overline{\Delta\delta}_{CSGT}$ = 16.3 ppm), the GIAO method correlates better with the experimental results than the CSGT method for the calculation of the ^{19}F magnetic shieldings at this level of theory ($\overline{R}^2_{GIAO} = 0.834$, $\overline{R}^2_{CSGT} = 0.763$).

Analysis of ^{1}H Computational Results. In the *a*, *b*, and *d* structures the ethoxyl eclipses the C(2)H_B proton (Figure 8b), and interestingly, in these three cases this proton is less deshielded than C(2)H_A. From the optimized geometries it can easily be seen that the *c* structure is the only one in which, along the C(1)−C(2) bond, the ethoxyl does not eclipse any of the diastereotopic protons (Figure 8c). This observation may explain why the order of deshieldings of the C(2)H_2 protons is inverted only in this latter structure, although the actual order does not agree with that which would be expected from the consideration of the through-space deshielding effect of the neighboring oxygen. A linear trend similar to that found for the fluorine resonances might be obscured by a concomitant effect resulting from the C(3) halogens and/or other through-bond mechanisms weighed by conformational variations. Furthermore, it is noteworthy that the most sterically hindering aliphatic chains (R^1 and R^2 in Figure 8b,c) do not adopt the *anti* positions (average dihedral angle of 119.35°). It is interesting to note that the largest differentiation (>1 ppm) between both diastereotopic C(2)H_2 protons is predicted for the *b* structure, in which the ethoxyl and the chlorine are found on the same side, and the C(2)H_B between them is the most deshielded proton resonance predicted.

As seen for the ^{19}F NMR, the B set of experimental resonances appears to show better correlation with all of the simulated systems (0.997 vs 0.983 for the GIAO/*a*, see Supporting Information). The *a* structure appears to exhibit better correlation with the A pattern for both methods whereas either *a*, *c*, or *d* correlates much better than *b* with B for both methods. The GIAO method gives a slightly better average correlation with the experimental results ($\overline{R}^2_{GIAO} = 0.957$, $\overline{R}^2_{CSGT} = 0.935$) and a smaller systematic error ($\overline{\Delta\delta}_{GIAO} = 0.17$ ppm, $\overline{\Delta\delta}_{CSGT} = -2.7$ ppm) than the CSGT method for the calculation of the ^{1}H magnetic shieldings at this level of theory.

Analysis of ^{13}C Computational Results. With the exception of the GIAO result for the *b* structure in which the C(4) and C(3) are inverted, for all of the four structures considered the same order of carbon shieldings given by the experimental assignment is found by both methods. Both methods also agree in finding the *c* structure to correlate much better and with a very similar quality, with both the A and B sets of resonances (see Supporting Information for data). Given a smaller systematic error ($\overline{\Delta\delta}_{GIAO}$ = 22.4 ppm, $\overline{\Delta\delta}_{CAGT}$ = 3.1 ppm) and a slightly better average correlation ($\overline{R}^2_{GIAO}$ = 0.988, $\overline{R}^2_{CSGT} = 0.992$) with the experimental results, the CSGT seems to be the first choice for the calculations of magnetic shieldings of ^{13}C nuclei at this level of theory.

Conclusions

The poly(CTFE-*co*-EVE) copolymer was characterized using high-resolution solution-state NMR spectroscopy. Broad signals resulting from the overlapping of different chemical shifts were observed in all spectra and explained as a consequence of a complex mixture of diastereomerically related compounds. A computational study of the isotropic magnetic shieldings at the DFT level of theory with the GIAO and CSGT methods supports the experimental assignment showing that the structures *a*, *b*, *c*, and *d* are representative of the stereochemical variety of the real sample.

The computational results indicate the C(1) configuration to be the main factor in the discrimination in the real sample between the A and B sets of resonances. Furthermore, the dihedral angles between the groups of interest in the geometry-optimized structures, i.e., C(4)−C(1) and C(1)−C(2) substituents, always adopted a staggered and an eclipsed conformation, respectively, and that the eclipsed form had the most sterically hindering aliphatic chains far from the expected *anti* positions. The C(3) configuration, being determined by two halogen substituents, has a far smaller influence on the shieldings of the diastereotopic nuclei. End groups of the poly(CTFE-*co*-EVE) copolymer are suggested but due to poor resolution no quantitative values could be deduced. Such results are important to enable further characterizations of poly(CTFE-*alt*-VEs) copolymers or poly(CTFE-*co*-HFP-*alt*-VEs) terpolymers as potential precursors of polymer electrolytes for fuel cell membranes.[36]

Supporting Information Available: ^{1}H- and ^{19}F-coupled and nondecoupled ^{1}H and ^{19}F 1D spectra, discussion of end groups with the ^{1}H−^{13}C HSQC spectrum expanded on the aliphatic region, the ^{1}H−^{13}C HMBC spectrum and its expansion on the aliphatic region, the ^{19}F COSY spectrum, tables of computational results. This material is available free of charge via the Internet at http://pubs.acs.org.

References and Notes

(1) Ameduri, B.; Boutevin, B. *Well-Architectured Fluoropolymers: Synthesis, Properties and Applications*; Elsevier Science: Amsterdam, 2004.
(2) Thomas, W. M.; O'Shaughnessy, T. *J. Polym. Sci.* **1953**, *11*, 455–470.
(3) Garbuglio, C.; Ragazzini, M.; Pilate, O.; Carcano, D.; Ceridalli, G. B. *Eur. Polym. Mater.* **1967**, *3*, 137–144.
(4) Tabata, Y.; Du Plessis, T, A. *J. Polym. Sci., Part 1A* **1971**, *9A*, 3425–3435.
(5) Hisasue, M.; Ichimura, M.; Kodama, S.; Miyake, H. Asahi Glass Co Ltd., FR 2 378 806, **1978**; Chem. Abstr. 80, 165070.
(6) Hisasue, M.; Kojima, G.; Kojima, H. Asahi Glass Co Ltd., P 54 163 985, **1979**; Chem. Abstr. 92, 182351.
(7) Nakano, Y.; Miyazaki, H.; Watanabe, K. Asahi Glass Co Ltd., P 62 073 944, **1987**; Chem. Abstr., 107, 98345.
(8) Takakura, T. CTFE/Vinyl Ether Copolymers. In Schiers, J., Ed.; *Modern Fluoropolymers*; Wiley: New York, 1997; Vol. *29*, p 557.
(9) Gaboyard, M.; Hervaud, Y.; Boutevin, B. *Polym. Int.* **2002**, *51*, 577–584.
(10) Russo, S.; Behari, K.; Chengi, S.; Pianca, M.; Barchiesi, E.; Moggi, G. *Polymer* **1993**, *34*, 4777−4781.
(11) Pianca, M.; Barchiesi, E.; Esposto, E.; Radice, S. J. *J. Fluorine Chem.* **1999**, *95*, 71–84.
(12) Wormald, P.; Apperley, D. C.; Beaume, F.; Harris, R. K. *Polymer* **2003**, *44*, 643–651.
(13) Macheteau, J. P.; Oulyadi, H.; van Hemelryc, B.; Bourdonneau, M.; Davoust, D. *J. Fluorine Chem.* **2000**, *104*, 149–154.
(14) Battiste, J.; Newmark, R. A. *Prog. NMR Spectrosc.* **2006**, *48*, 1–23.
(15) Battiste, J.; Jing, N. Y.; Newmark, P. A. *J. Fluorine Chem.* **2004**, *125*, 1331–1337.
(16) Boyer, C.; Valade, D.; Lacroix-Desmazes, P.; Ameduri, B.; Boutevin, B. *J. Polym. Sci., Part A: Polym. Chem.* **2006**, *44*, 5763−5777.
(17) Mladenov, G.; Ameduri, B.; Kostov, G.; Mateva, R. *J. Polym. Sci., Part A: Polym. Chem.* **2006**, *44*, 1470–1485.
(18) Duc, M.; Ameduri, B.; Boutevin, B.; Kharroubi, M.; Sage, J.-M. *Macromol. Chem. Phys.* **1998**, *199*, 1271–1289.

(19) Wormald, P.; Ameduri, B.; Harris, R. K.; Hazendonk, P. *Polymer* **2008**, *49*, 3629–3638.
(20) Mason, J. *Multinuclear NMR*; Plenum Press: New York, 1987; pp 442−445.
(21) Raulet, R.; Grandclaude, D.; Humbert, F.; Canet, D. *J. Magn. Reson*. **1997**, *124* (1), 259–262.
(22) Schwarz, R.; Seelig, J.; Kunnecke, B. *Magn. Reson. Chem*. **2004**, *42* (6), 512–517.
(23) Jones, B. G.; Branch, S. K.; Threadgill, M. D.; Wilman, D. E. V. *J. Fluorine Chem*. **1995**, *74*, 221–222.
(24) Bailey, W. I.; Kotz, A. L.; McDaniel, P. L.; Parees, D. M.; Schweighardt, F. K.; Yue, H. J.; Anklin, C. *Anal. Chem*. **1993**, *65*, 752−758.
(25) Lu, J.; Claude, J.; Zhang, Q.; Wang, Q. *Macromolecules*. **2006**, *39*, 6962–6968.
(26) Frisch, M. J.; Trucks, G. W.; Schlegel, H. B.; Scuseria, G. E.; Robb, M. A.; Cheeseman, J. R.; Montgomery Jr., J. A.; Vreven, T.; Kudin, K. N.; Burant, J. C.; Millam, J. M.; Iyengar, S. S.; Tomasi, J.; Barone, V.; Mennucci, B.; Cossi, M.; Scalmani, G. Rega, N.; Petersson, G. A.; Nakatsuji, H.; Hada, M.; Ehara, M.; Toyota, K.; Fukuda, R.; Hasegawa, J.; Ishida, M.; Nakajima, T.; Honda, Y.; Kitao, O.; Nakai, H.; Klene, M.; Li, X.; Knox, J. E.; Hratchian, H. P.; Cross, J. B.; Bakken, V.; Adamo, C.; Jaramillo, J.; Gomperts, R.; Stratmann, R. E.; Yazyev, O.; Austin, A. J.; Cammi, R.; Pomelli, C.; Ochterski, J. W.; Ayala, P. Y.; Morokuma, K.; Voth, G. A.; Salvador, P.; Dannenberg, J. J.; Zakrzewski, V. G.; Dapprich, S.; DanielsA. D.; Strain, M. C.; Farkas, O.; Malick, D. K.;. Rabuck, A. D.; Raghavachari, K.; Foresman, J. B.; Ortiz, J. V.; Cui, Q.; Baboul, A. G.; Clifford,V.; Cioslowski, J.; Stefanov, B. B.; Liu, G.; Liashenko, A.; Piskorz, P.; Komaromi, I.; Martin, R. L.; Fox, D. J.; Keith, T. Al-Laham, M. A.; Peng, C. Y.; Nanayakkara, A.; Challacombe, M.; Gill, P. M. W.; Johnson, B.; Chen, W.; Wong, M. W.; Gonzalez, C.; Pople, J. A. *Gaussian 03, Revision B.05*, Gaussian Inc.: Wallingford, CT, 2003.
(27) Tiers, G. V. D.; Bovey, F. A. *J. Polym. Sci., Part A-1* **1963**, 833–841.
(28) Boutevin, B.; Cersosimo, F.; Youssef, B. *Macromolecules* **1992**, *25*, 2842–2846.
(29) Beaune, O.; Bessiere, J. M.; Boutevin, B.; El Bachiri, A. *J. Fluorine Chem*. **1995**, *73*, 27–32.
(30) Tanuma, K.; Ohnishi, H.; Okamoto, S.; Morikawa, K. *J. Fluorine Chem*. **1996**, *76*, 45–48.
(31) Kurtkaya, S.; Barone, V.; Peralta, J. E.; Contreras, R. H.; Snyder, J. P. *J. Am. Chem. Soc*. **2002**, *124*, 9702−9703.
(32) Holstein, P.; Scheler, U.; Harris, R. K. *Magn. Reson. Chem*. **1997**, *35*, 647–649.
(33) Cheeseman, J. R.; Trucks, G. W.; Keith, T. A.; Frisch, M. J. *J. Chem. Phys*. **1995**, *104*, 5497–5509.
(34) Jackman, L. M.; Sternhell, S. *Applications of Magnetic Resonance Spectroscopy in Organic Chemistry*; Pergamon Press: Oxford, 1969; p 71.
(35) San Fabian, J.; Westra Hoekzema, A. J. A. J. *J. Chem. Phys*. **2004**, *121*, 5258−6276.
(36) Valade, D.; Boschet, F.; Ameduri, B., submitted to *Macromolecules*.